# Toppling the Transport Properties with Cationic Overstoichiometry in Thermoelectric Colusite: [Cu 26 Cr 2 Ge 6 ] 1+$\delta$ S 32

Gabin Guelou, Ventrapati Pavan Kumar, Abdelhamid Bourhim, Pierric Lemoine, Bernard Raveau, Andrew R. Supka, Oleg Lebedev, Rabih Al Rahal Al Orabi, Marco Fornari, Koichiro Suekuni, et al.

# Toppling the transport properties with cationic over-stoichiometry in thermoelectric colusite, $[Cu_{26}Cr_2Ge_6]_{1+\delta}S_{32}$

*Gabin Guélou,[‡,a] Ventrapati Pavan Kumar,[‡,a] Abdelhamid Bourhim,[a] Pierric Lemoine,[b] Bernard Raveau,[a] Andrew Supka,[c] Oleg I. Lebedev,[a] Rabih Al Rahal Al Orabi,[c,e] Marco Fornari,[c] Koichiro Suekuni,[d] Emmanuel Guilmeau[*,a]*

[a] CRISMAT, CNRS, Normandie Univ, ENSICAEN, UNICAEN, 14000 Caen, France.

[b] Univ Rennes, CNRS, ISCR – UMR 6226, F-35000 Rennes, France.

[c] Department of Physics and Science of Advanced Materials Program, Central Michigan University, Mt. Pleasant, MI 48859, USA.

[d] Department of Applied Science for Electronics and Materials, Interdisciplinary Graduate School of Engineering Sciences, Kyushu University, Kasuga, Fukuoka 816-8580, Japan.

[e] Solvay, Design and Development of Functional Materials Department, Axel'One, 87 avenue des Frères Perret, 69192 Saint Fons, Cedex, France

**Keywords**

Thermoelectric, sulfide, colusite, off-stoichiometry, conductive network, transport mechanism

**Abstract**

The excellent thermoelectric properties of colusite are known to be closely related to the nature of the cations at the core of the tetrahedral-octahedral complexes. Here, we demonstrate that cation over-stoichiometry decreases the carrier concentration and also generates structural disorder, which modify the conduction mechanism in a way that resembles the effect of cation-size mismatch. This functionalization of the "$Cu_{26}S_{32}$" conductive network leads to a high figure of merit of 1.0 at 700 K. This study highlights the importance of the cationic arrangement and furthers our understanding on the fascinating transport properties in colusite.

Thermoelectricity (TE) has been considered as a potential source of energy for the past decades, in particular following the reports of materials with relatively high efficiency.[1] This efficiency can be characterized by the figure of merit, $ZT = S^2T/\rho\kappa$, which needs to be maximized by balancing conflicting electronic and thermal transport properties: a high Seebeck coefficient, $S$, a low electrical resistivity, $\rho$ (to maximize the power factor $PF = S^2/\rho$), and a low thermal conductivity, $\kappa$. Unfortunately, most performing materials involve difficult synthesis routes and/or toxic and expensive elements that critically limit their large-scale production.[2–4] There is nonetheless a host of potential applications that can be reached if we can obtain good performances in bulk materials prepared from earth-abundant elements.[5] Among the promising groups of materials, ternary and quaternary copper sulfides have attracted considerable attention,[6] with many reports of favorable raw material cost-to-efficiency ratio. Promising compositions include bornite $Cu_5FeS_4$,[7–9] germanite derivative $Cu_{22}Fe_8Ge_4S_{32}$,[10,11] stannoidite $Cu_{8.5}Fe_{2.5}Sn_2S_{12}$,[12] $Cu_2SnS_3$,[13] kesterite $Cu_2ZnSnS_4$,[14,15] $Cu_4Sn_7S_{16}$,[16] $CuFeS_2$[17], tetrahedrites $Cu_{12-x}T_xSb_4S_{13}$ ($T$ = Mn, Fe, Ni, Zn)[18–21] and colusites $Cu_{26}T_2M_6S_{32}$ ($T$ = V, Nb, Ta, Cr, Mo, W; $M$ = Sn, Ge).[22–30]

In previous reports, the peculiar behavior of the electrical transport properties in colusite, in particular in $Cu_{26}Cr_{2-x}T_xGe_6S_{32}$ ($T$ = Mo, W)[29,30] and $Cu_{26}(V,Nb)_2Sn_6S_{32}$[25–27] was investigated in details and revealed the importance of cationic ordering/disordering on the electrical and thermal transport properties. In $Cu_{26}Cr_2Ge_6S_{32}$, exceptional transport properties ($PF$ = 1.94 mW m$^{-1}$ K$^{-2}$ at 700 K) were recently reported and explained by the presence of interstitial Cr cations forming mixed tetrahedral-octahedral $[CrS_4]Cu_6$ complexes, which influence the geometry of the conductive "$Cu_{26}S_{32}$" framework. Our previous analysis of the colusite structure[29] showed that it derives from the sphalerite and consequently offers various tetrahedral cavities for hosting additional cations. Such structural properties should make possible the realization of cationic over

stoichiometry with disorder and consequently has a great potential for changing its transport properties. The effect of deviation from ideal stoichiometry was shown in $Cu_{26}(V,Nb)_2Sn_6S_{32}$[25–27] by sulfur volatilization using high-temperature sintering processes: cationic over-stoichiometry associated with atomic-scale defects/disordered states, including interstitial defects, anti-site defects, and site splitting was achieved. In particular, a high concentration of antisite defects decreases the thermal conductivity drastically, and consequently increased the ZT significantly.[26] However, this sulfur volatilization process cannot be applied to $Cu_{26}Cr_2Ge_6S_{32}$ due to its lower thermal stability.[28] For this reason, we have investigated samples with global cationic composition larger than that corresponding to the ideal formula but working at lower temperature.

We report herein on the effect of the cationic over-stoichiometry in the series $[Cu_{26}Cr_2Ge_6]_{1+\delta}S_{32}$ on the carrier concentration and conduction mechanism together with the formation of structural defects. Our results, supported by first principles calculations, indicate that excess cations are likely to be interstitial Cu with the overall consequence of moderately improving the thermoelectric efficiency.

Samples with composition $[Cu_{26}Cr_2Ge_6]_{1+\delta}S_{32}$ ($\delta = 0$, 0.0159, 0.0240 and 0.0323), were prepared via mechanical alloying of the precursors followed by Spark Plasma Sintering (SPS). Mechanically alloyed powders show no obvious traces of secondary phases and overall poor crystallinity. After consolidation at 600°C using SPS, the crystallographic structure of colusite has been confirmed by Rietveld refinement of high-resolution Powder X-ray Diffraction (PXRD) data (Fig. S1-S2 and Table S1-S2 of the supporting information). Analysis of the patterns revealed traces (*ca*. 2 wt%) of a $Cu_8GeS_6$ ($Pmn2_1$, $a$ = 7.04 Å, $b$ = 6.97 Å, $c$ = 9.87 Å) secondary phase only in the off-stoichiometric samples $[Cu_{26}Cr_2Ge_6]_{1+\delta}S_{32}$, where $\delta$ = 0.0159 and 0.0323. Rietveld refinements (Fig. S1-S2) indicate equivalent unit cell parameters and atomic coordinates for both pristine and

off-stoichiometry colusites (Table S1-S2). Consequently, no obvious deviation from the structural model of pristine colusite can be established for the $[Cu_{26}Cr_2Ge_6]_{1+\delta}S_{32}$ series using PXRD only. SEM/EDS analyses on polished surfaces confirmed the presence of Cu-S binary impurity in $[Cu_{26}Cr_2Ge_6]_{1+\delta}S_{32}$ ($\delta$ = 0.0159 and 0.0323) and the otherwise good homogeneity in the cationic ratios for all samples (Fig. S3-S6, Table S3). It is unlikely that sulfur deficiency in the initial composition would translate into sulfur vacancies in the crystallized phase. Rather, it is more sensible to consider the off-stoichiometric colusite as a cation rich phase where the many available interstitials are randomly occupied by a small fraction of excess cations. The presence of such partially filled interstitials, combined with the presence of disordered domains, has been demonstrated recently by Suekuni *et al.*[27] in $Cu_{26}Nb_2Sn_6S_{32}$ and a more thorough investigation of the cationic repartition in high-performance $Cu_{26}V_2Sn_6S_{32}$ colusite is currently on-going. To support the experimental evidence, we have computed with first principles method the formation energy for sulfur vacancies as well as for Ge, Cr, and Cu interstitial. The results (Table 1) indicate that easy-to-form defects are Cu interstitials while S vacancies and other interstitials are less favored.

**Table 1** Formation energy (in eV) of defects with respect to the formation energy of the pristine crystal. The values were computed assuming one defect per cell (comparable to $\delta$ = 0.0323). Effects associated to defect-defect interaction were investigated but found not significant. The two values associated with each defect correspond to different position for the vacancy or the interstitial within the unit cell.

| | S vacancy | Cu interstitial | Cr interstitial | Ge interstitial |
|---|---|---|---|---|
| 24i/8e | 1.825/3.018 | - | - | - |
| 24i/6d | - | 0.694/0.789 | 1.907/2.288 | 1.993/2.405 |

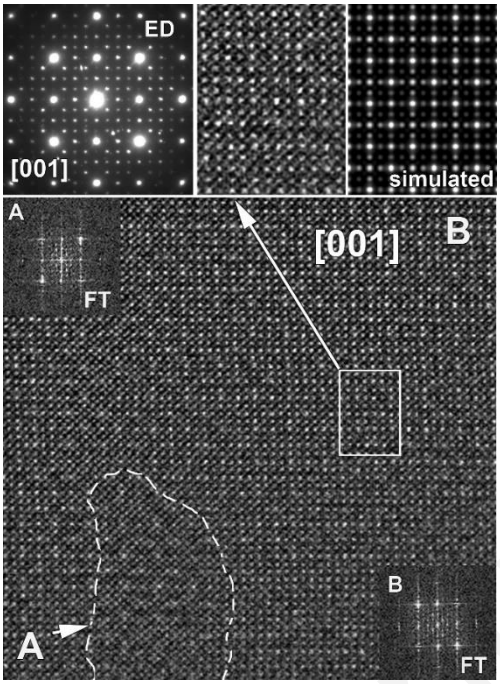


**Figure 1.** High resolution HAADF-STEM image of $[Cu_{26}Cr_2Ge_6]_{1.024}S_{32}$ (cubic, $P\bar{4}3n$) for the [001] zone with the corresponding electron diffraction (ED) pattern, enlarged ordered domain and simulated HAADF-STEM image. The regions marked as A and B correspond to disordered and relatively ordered domains respectively with corresponding FT patterns given as insets.

In order to get insights in the level of disorder induced by cation over-stoichiometry at a local scale, transmission electron microscopy (TEM), including electron diffraction analysis (ED) and high-angular annular dark field scanning TEM (HAADF-STEM) were performed. When comparing HAADF-STEM micrographs taken on the pristine sample reported previously[29] and the over-stoichiometric $[Cu_{26}Cr_2Ge_6]_{1.024}S_{32}$, we noticed the presence of ordered (see B region in Fig. 1) but also additional areas exhibiting significant levels of disorder (see A region in Fig. 1). Furthermore, in the ordered B domains, while no interstitial cations could be observed unequivocally, clear variations in the contrast, and particularly in brightness of atomic columns, evidence significant levels of cationic rearrangement, as opposed to pristine $Cu_{26}Cr_2Ge_6S_{32}$. These findings echo the observations made on $Cu_{26}V_2Sn_6S_{32}$ when sulfur deficiency was induced by high

processing temperatures[25] and confirm that temperature-induced cationic disorder could be somehow reproduced in the less thermally stable $Cu_{26}Cr_2Ge_6S_{32}$. A noticeable difference is found in the evolution of the lattice parameter, *a*, that remains unchanged in the present study, in opposition with the large increase observed in $Cu_{26}V_2Sn_6S_{32}$ with sintering temperature. Very recently, we demonstrated that the large reduction in thermal conductivity in $Cu_{26}V_2Sn_6S_{32}$, while it is temperature-induced, is caused by a higher concentration of anti-site defects rather than introducing vacancies or interstitial atoms. The rather unchanged lattice parameter here might suggest that the concentration of anti-site defects is lower than in thermally disordered $Cu_{26}V_2Sn_6S_{32}$.[26]

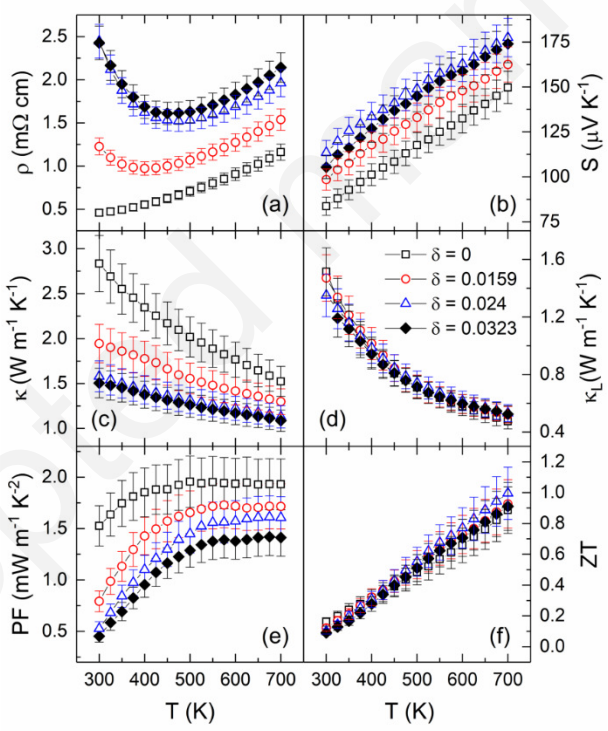


**Figure 2.** Temperature dependence of the (a) electrical resistivity ($\rho$), (b) Seebeck coefficient ($S$), (c) thermal conductivity ($\kappa$), (d) lattice thermal conductivity ($\kappa_L$), (e) power factor ($PF$), and (f) figure of merit $ZT$ in the $[Cu_{26}Cr_2Ge_6]_{1+\delta}S_{32}$ series.

The electrical and thermal transport properties of $[Cu_{26}Cr_2Ge_6]_{1+\delta}S_{32}$ ($\delta$ = 0, 0.0159, 0.024 and 0.0323), over the temperature range $300 \leq T\,(K) \leq 700$, are compiled in Fig. 2. With cation over-

stoichiometry, the Seebeck coefficient steadily increases over the investigated temperature range and reaches a maximum of 175 μV $K^{-1}$ at 700 K for $\delta \geq 0.024$, Fig. 2(b). All samples thus retain a *p*-type character with holes as majority charge carriers. Meanwhile, the electrical resistivity evolves with cation over-stoichiometry in a way reminiscent of that of $Cu_{26}Cr_{2-x}T_xGe_6S_{32}$ (*T* = Mo, W) solid solutions.[30] Indeed, the presence of an excess cation dramatically changes the temperature behavior of the electrical resistivity, in particular with the apparition of an upturn from a semiconducting to a metallic T-dependence at *ca*. 400-500 K, Fig. 2(a). This effect was linked to the disorder caused by cation-size mismatch on the 2*a* site;[30] however, in the present case, there is also a change in the charge carrier concentration from the filling of initially vacant interstitial sites by extra cations in the off-stoichiometric samples. As a consequence, the amplitude of the electrical resistivity and the Seebeck coefficient also changes significantly, as opposed to converging toward the same values as it was the case with isovalent substitution.[30] Instead, both the Seebeck coefficient and the electrical resistivity increase with cation over-stoichiometry, resulting in a power factor that steadily decreases with increasing off-stoichiometry over the whole investigated temperature range (Fig. 2(e)). Nonetheless, the electrical performance remains high for a copper-based sulfide with a maximum power factor of *ca*. 1.9 mW $m^{-1}$ $K^{-2}$ and *ca*. 1.4 mW $m^{-1}$ $K^{-2}$ at 700 K for pristine Cr-Ge colusite and $[Cu_{26}Cr_2Ge_6]_{1.0323}S_{32}$, respectively.

Such high performance in a thermoelectric sulfide is scarce and the transport mechanisms in colusite are well worth investigating. Hence, low-temperature Seebeck coefficient and electrical and thermal conductivities were measured down to 5 K for $[Cu_{26}Cr_2Ge_6]_{1+\delta}S_{32}$ ($\delta$ = 0, 0.0159, 0.024) (Fig. S7). As expected from the presence of cation interstitials, the simultaneous increase of the Seebeck coefficient and the electrical resistivity in $[Cu_{26}Cr_2Ge_6]_{1+\delta}S_{32}$ ($\delta$ = 0.0159, 0.024) compared to pristine compound is consistent with a reduced charge carrier concentration. This is

confirmed by low-temperature Hall effect measurements (inset in Fig. 3) with a 3 times lower concentration at 5 K for the cation-rich colusites. The temperature dependence of the electrical resistivity is semiconducting for $[Cu_{26}Cr_2Ge_6]_{1+\delta}S_{32}$ ($\delta$ = 0.0159, 0.024) down to *ca*. 100 K (Fig. S7(a)) as expected from the trend observed in Fig. 2 (a). Below 100 K, the temperature dependence of both Seebeck coefficient and electrical resistivity changes radically for $[Cu_{26}Cr_2Ge_6]_{1+\delta}S_{32}$ ($\delta$ = 0.0159, 0.024) while pristine $Cu_{26}Cr_2Ge_6S_{32}$ remains in a typical metallic regime (Fig. S7).

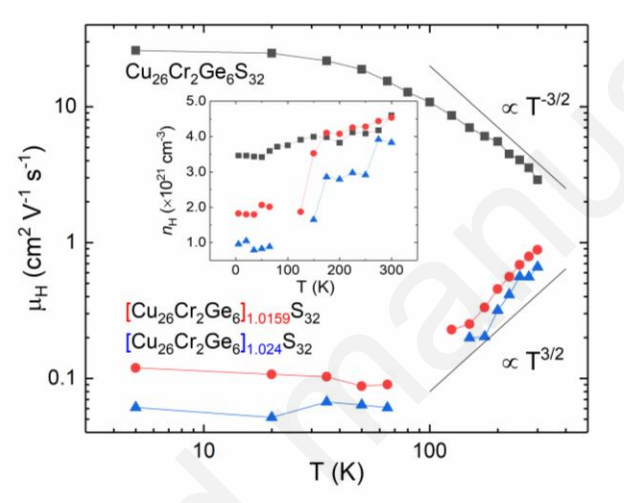


**Figure 3.** Temperature dependence of the Hall mobility for $Cu_{26}Cr_2Ge_6S_{32}$, $[Cu_{26}Cr_2Ge_6]_{1.0159}S_{32}$ and $[Cu_{26}Cr_2Ge_6]_{1.024}S_{32}$ with the charge carrier concentration shown as an inset.

Once again, this behavior resembles that of $Cu_{26}Cr\mathit{T}Ge_6S_{32}$ ($T$ = Mo, W) compounds with a nonetheless clear change in the temperature dependence of the Seebeck coefficient at 112 K,[30] that may have been revealed by the lower carrier concentration in the present study. Indeed, in the case of the aforementioned solid solutions, the isovalent doping in samples had kept the low-temperature Seebeck coefficient rather low, close to (or lower than) that of pristine Cr-Ge colusite.[30] The low resulting Seebeck coefficient followed a nearly linear temperature dependence below 300 K that may have been occulting the transition. This further suggests that the observed

change in conduction mechanisms is unrelated to microscopic features such as grain boundary, as we would not expect the Seebeck coefficient to exhibit such a marked transition. The peculiar behavior of the electrical resistivity between *ca*. 100 K and *ca*. 500 K can be associated (as it was demonstrated for the solid solutions) to chemical disorder, chemical localization, and/or variable range hopping (VRH) conductivity.[30] Indeed, the temperature dependence of the Hall mobility, Fig. 3, switches over 100 K from typical acoustic phonon scattering ($\propto T^{-3/2}$) for pristine colusite to an ionized impurity scattering type dependence ($\propto T^{3/2}$) for the off-stoichiometric compound. Additionally, the signal from Hall effect measurements at temperatures around the transition is disturbed by an anomalous contribution that is responsible for the few data points missing in Fig. 3. The relationship between this contribution and the changes in transport properties is undoubtedly complex and well worth further investigation that falls outside the scope of this study. As with the solid solutions, the slope of $d\rho/dT$ changes sign around 100 K for the samples with extra cations, suggesting that the change in scattering mechanism also leads to an intermediate state between an insulating and metallic regime.

As pointed out beforehand and in our previous work,[30] the cation-size mismatch in the 2*a* position is responsible for a similar change of mechanism, only this time it is accompanied by a change in the charge carrier concentration. This suggests that cations occupying other initially empty interstitial sites, with chemical environment rather similar to that of the 2*a* position, and cationic disorder are extremely efficient in altering the conduction mechanism. The electrical transport properties of colusite, insured by the "$Cu_{26}S_{32}$" conductive framework,[29,30] can therefore be altered in a relatively similar fashion by either cation-size mismatch on the 2*a* site or cation over-stoichiometry. In other words, the cationic arrangement necessary to ensure a metallic

behavior and classical acoustic phonon scattering in pristine $Cu_{26}Cr_2Ge_6S_{32}$, is markedly upset by a slight cationic over-stoichiometry.

In order to complete the investigation of the thermoelectric performances of $[Cu_{26}Cr_2Ge_6]_{1+\delta}S_{32}$, the thermal conductivity was determined (Fig. 2(c)) and the lattice contribution was extracted using Wiedemann-Franz law (Fig. 2(d)). Overall, a clear diminution in the thermal conductivity was obtained from cation over-stoichiometry, in particular at the lower end of the investigated temperature range. A minimum at room temperature was determined for $[Cu_{26}Cr_2Ge_6]_{1+\delta}S_{32}$ ($\delta \geq 0.024$) with *ca*. 1.5 W m $K^{-1}$, a nearly 100 % decrease from pristine $Cu_{26}Cr_2Ge_6S_{32}$. At 700 K, the total thermal conductivity is decreased to *ca*. 1.1 W m $K^{-1}$ for $[Cu_{26}Cr_2Ge_6]_{1+\delta}S_{32}$ ($\delta \geq 0.024$). The origin of this diminution is rather clear with no apparent change in the lattice contribution to the thermal conductivity (Fig. 2(d)). The diminution in the electrical resistivity is thus mainly responsible for the observed reduction. This is also true at low-temperature where the significant drop in thermal conductivity is mainly attributed to a decrease in the electronic contribution (Fig. S7c). This contrasts with the observations made on the V-Sn colusite, where order/disorder domains observed by HAADF-STEM, similar to those observed in $[Cu_{26}Cr_2Ge_6]_{1.024}S_{32}$ (Fig. 1) were initially held responsible for a large decrease in the lattice contribution to the thermal conductivity.[25] This suggests that the disorder induced by cation over-stoichiometry, in contrast with high-temperature treatment, does not modify the distribution of cations enough so that the concentration of anti-site defects increases significantly, and thus does not shorten the acoustic phonon lifetimes. This is further supported by the absence of significant evolution in the unit cell parameter, *a*, in $[Cu_{26}Cr_2Ge_6]_{1+\delta}S_{32}$. While some traces of secondary phase were found in some samples, they do not seem to have any impact of the lattice thermal conductivity at high temperature. Consequently, the calculated figure of merit is mildly improved at high temperature

with a maximum ZT of 1.0 at 700 K for $[Cu_{26}Cr_2Ge_6]_{1.024}S_{32}$, (Fig. 2f), the highest reported value in colusites to date. It is important to note that achieving ultra-low lattice thermal conductivity ($\kappa_{lat}$ ≈ 0.2 W m$^{-1}$ K$^{-1}$) in Cr-Ge colusite, as we demonstrated was possible in $Cu_{26}V_2Sn_6S_{32}$, remains an open challenge and would lead to figure of merit values well over unity.

We have demonstrated that the presence of a slight excess of cations had an impact on the "$Cu_{26}S_{32}$" conductive framework by simultaneously altering the charge carrier concentration and the conduction mechanism in colusite, $[Cu_{26}Cr_2Ge_6]_{1+\delta}S_{32}$. Many interstitial sites are available for the additional cations with a chemical environment similar to the 2*a* position, namely a particular tetrahedral-octahedral complex with competing ionic and metallic bonds. Additionally, this excess cation causes significant level of cationic rearrangement, as evidenced by HAADF-STEM. However, the exact nature of the cations in the interstitial positions and their possible repartition is yet to be elucidated using powerful structural investigation tools such as synchrotron and/or neutron diffraction. Overall, along with a moderate improvement in the thermoelectric response, these findings open new ways for improvement via simultaneous charge carrier doping and transport mechanism modulation in copper sulfides.

**Supporting Information**

The following file is available free of charge.

Supplementary_Information.pdf: Including the experimental section (p. S-1 to S-5); PXRD patterns and corresponding Rietveld refinements; elemental mappings; low-temperature electrical resistivity, Seebeck coefficient and thermal conductivity measurements.

**Corresponding Author**

* Emmanuel.guilmeau@ensicaen.fr

**Author Contributions**

The manuscript was written through contributions of all authors. All authors have given approval to the final version of the manuscript. ‡These authors contributed equally.

**Funding Sources**

ANR-15-CE05-0027

DOD-ONR (Grants N000141310635 and N000141512266).

**Acknowledgement**

The authors would like to thank Christelle Bilot and Jerôme Lecourt for technical support and the financial support of the French Agence Nationale de la Recherche (ANR-15-CE05-0027), FEDER and Region Normandy. K.S. thanks the International Joint Research Program for Innovative Energy Technology funded by the Ministry of Economy, Trade and Industry (METI), Japan. M.F. and A.R.S. acknowledge collaboration with the AFLOW Consortium (http://www.aflow.org) under the sponsorship of DOD-ONR (Grants N000141310635 and N000141512266).

**Abbreviations**

SPS, spark plasma sintering; PXRD, powder x-ray diffraction; SEM/EDS, scanning electron microscopy with energy-dispersive x-ray spectroscopy; ED, electron diffraction; TEM, transmission electron microscopy; HAADF-STEM, high-angular annular dark field scanning transmission electron microscopy.

**References**

(1) He, J.; Tritt, T. M. Advances in Thermoelectric Materials Research: Looking Back and

Moving Forward. *Science.* **2017**, *357*, eaak9997. https://doi.org/10.1126/science.aak9997.

(2) Biswas, K.; He, J.; Zhang, Q.; Wang, G.; Uher, C.; Dravid, V. P.; Kanatzidis, M. G. Strained Endotaxial Nanostructures with High Thermoelectric Figure of Merit. *Nat. Chem.* **2011**, *3*, 160–166. https://doi.org/10.1038/nchem.955.

(3) Biswas, K.; He, J.; Blum, I. D.; Wu, C.-I.; Hogan, T. P.; Seidman, D. N.; Dravid, V. P.; Kanatzidis, M. G. High-Performance Bulk Thermoelectrics with All-Scale Hierarchical Architectures. *Nature* **2012**, *489*, 414–418. https://doi.org/10.1038/nature11439.

(4) Pei, Y.; Shi, X.; Lalonde, A.; Wang, H.; Chen, L.; Snyder, G. J. Convergence of Electronic Bands for High Performance Bulk Thermoelectrics. *Nature* **2011**, *473* (7345), 66–69. https://doi.org/10.1038/nature09996.

(5) Freer, R.; Powell, A. V. Realising the Potential of Thermoelectric Technology: A Roadmap. *J. Mater. Chem. C* **2020**, *8* (2), 441–463. https://doi.org/10.1039/c9tc05710b.

(6) Powell, A. V. Recent Developments in Earth-Abundant Copper-Sulfide Thermoelectric Materials. *J. Appl. Phys.* **2019**, *126* (10), 100901. https://doi.org/10.1063/1.5119345.

(7) Qiu, P.; Zhang, T.; Qiu, Y.; Shi, X.; Chen, L. Sulfide Bornite Thermoelectric Material: A Natural Mineral with Ultralow Thermal Conductivity. *Energy Environ. Sci.* **2014**, *7* (12), 4000–4006. https://doi.org/10.1039/c4ee02428a.

(8) Guélou, G.; Powell, A. V.; Vaqueiro, P. Ball Milling as an Effective Route for the Preparation of Doped Bornite: Synthesis, Stability and Thermoelectric Properties. *J. Mater. Chem. C* **2015**, *3* (40), 10624–10629. https://doi.org/10.1039/c5tc01704a.

(9) Pavan Kumar, V.; Barbier, T.; Lemoine, P.; Raveau, B.; Nassif, V.; Guilmeau, E. The

Crucial Role of Selenium for Sulphur Substitution in the Structural Transitions and Thermoelectric Properties of Cu5FeS4 Bornite. *Dalt. Trans.* **2017**, *46* (7), 2174–2183. https://doi.org/10.1039/c6dt04204j.

(10) Pavan Kumar, V.; Paradis-Fortin, L.; Lemoine, P.; Caignaert, V.; Raveau, B.; Malaman, B.; Le Caër, G.; Cordier, S.; Guilmeau, E. Designing a Thermoelectric Copper-Rich Sulfide from a Natural Mineral: Synthetic Germanite Cu22Fe8Ge4S32. *Inorg. Chem.* **2017**, *56* (21), 13376–13381. https://doi.org/10.1021/acs.inorgchem.7b02128.

(11) Pavan Kumar, V.; Paradis-Fortin, L.; Lemoine, P.; Le Caer, G.; Malaman, B.; Boullay, P.; Raveau, B.; Guélou, G.; Guilmeau, E. Crossover from Germanite to Renierite-Type Structures in Cu22-XZnxFe8Ge4S32 Thermoelectric Sulfides. *ACS Appl. Energy Mater.* **2019**, *2* (10), 7679–7689. https://doi.org/https://doi.org/10.1021/acsami.0c00094.

(12) Pavan Kumar, V.; Barbier, T.; Caignaert, V.; Raveau, B.; Daou, R.; Malaman, B.; Caër, G. Le; Lemoine, P.; Guilmeau, E. Copper Hyper-Stoichiometry: The Key for the Optimization of Thermoelectric Properties in Stannoidite Cu8+xFe3-XSn2S12. *J. Phys. Chem. C* **2017**, *121* (30), 16454–16461. https://doi.org/10.1021/acs.jpcc.7b02068.

(13) Shen, Y.; Li, C.; Huang, R.; Tian, R.; Ye, Y.; Pan, L.; Koumoto, K.; Zhang, R.; Wan, C.; Wang, Y. Eco-Friendly p-Type Cu2SnS3 Thermoelectric Material: Crystal Structure and Transport Properties. *Sci. Rep.* **2016**, *6*, 32501. https://doi.org/https://doi.org/10.1038/srep32501.

(14) Liu, M. L.; Huang, F. Q.; Chen, L. D.; Chen, I. W. A Wide-Band-Gap p -Type Thermoelectric Material Based on Quaternary Chalcogenides of Cu2ZnSnQ4 (Q=S,Se). *Appl. Phys. Lett.* **2009**, *94* (20), 202103. https://doi.org/https://doi.org/10.1063/1.3130718.

(15) Yang, H.; Jauregui, L. A.; Zhang, G.; Chen, Y. P.; Wu, Y. Nontoxic and Abundant Copper Zinc Tin Sulfide Nanocrystals for Potential High-Temperature Thermoelectric Energy Harvesting. *Nano Lett.* **2012**, *12* (2), 540–545. https://doi.org/10.1021/nl201718z.

(16) Bourgès, C.; Lemoine, P.; Lebedev, O. I.; Daou, R.; Hardy, V.; Malaman, B.; Guilmeau, E. Low Thermal Conductivity in Ternary Cu4Sn7S16 Compound. *Acta Mater.* **2015**, *97*, 180–190. https://doi.org/https://doi.org/10.1016/j.actamat.2015.06.046.

(17) Chen, D.; Zhao, Y.; Chen, Y.; Lu, T.; Wang, Y.; Zhou, J.; Liang, Z. Thermoelectric Enhancement of Ternary Copper Chalcogenide Nanocrystals by Magnetic Nickel Doping. *Adv. Electron. Mater.* **2016**, *2* (6), 1500473. https://doi.org/10.1002/aelm.201500473.

(18) Lu, X.; Morelli, D. T.; Xia, Y.; Zhou, F.; Ozolins, V.; Chi, H.; Zhou, X.; Uher, C. High Performance Thermoelectricity in Earth-Abundant Compounds Based on Natural Mineral Tetrahedrites. *Adv. Energy Mater.* **2013**, *3* (3), 342–348. https://doi.org/10.1002/aenm.201200650.

(19) Suekuni, K.; Tsuruta, K.; Kunii, M.; Nishiate, H.; Nishibori, E.; Maki, S.; Ohta, M.; Yamamoto, A.; Koyano, M. High-Performance Thermoelectric Mineral Cu 12-x Ni x Sb 4 S 13 Tetrahedrite. *J. Appl. Phys.* **2013**, *113* (4), 043712. https://doi.org/10.1063/1.4789389.

(20) Barbier, T.; Lemoine, P.; Gascoin, S.; Lebedev, O. I.; Kaltzoglou, A.; Vaqueiro, P.; Powell, A. V.; Smith, R. I.; Guilmeau, E. Structural Stability of the Synthetic Thermoelectric Ternary and Nickel-Substituted Tetrahedrite Phases. *J. Alloys Compd.* **2015**, *634*, 253–262. https://doi.org/10.1016/j.jallcom.2015.02.045.

(21) Barbier, T.; Rollin-Martinet, S.; Lemoine, P.; Gascoin, F.; Kaltzoglou, A.; Vaqueiro, P.;

Powell, A. V.; Guilmeau, E. Thermoelectric Materials: A New Rapid Synthesis Process for Nontoxic and High-Performance Tetrahedrite Compounds. *J. Am. Ceram. Soc.* **2016**, *99* (1), 51–56. https://doi.org/10.1111/jace.13838.

(22) Suekuni, K.; Kim, F. S.; Nishiate, H.; Ohta, M.; Tanaka, H. I.; Takabatake, T. High-Performance Thermoelectric Minerals: Colusites Cu 26 V 2 M 6 S 32 (M = Ge, Sn). *Appl. Phys. Lett.* **2014**, *105* (13), 132107. https://doi.org/10.1063/1.4896998.

(23) Suekuni, K.; Kim, F. S.; Takabatake, T. Tunable Electronic Properties and Low Thermal Conductivity in Synthetic Colusites Cu26-XZnxV2M6S 32 ($x \leq 4$, M = Ge, Sn). *J. Appl. Phys.* **2014**, *116* (6), 063706. https://doi.org/10.1063/1.4892593.

(24) Bourgès, C.; Gilmas, M.; Lemoine, P.; Mordvinova, N. E.; Lebedev, O. I.; Hug, E.; Nassif, V.; Malaman, B.; Daou, R.; Guilmeau, E. Structural Analysis and Thermoelectric Properties of Mechanically Alloyed Colusites. *J. Mater. Chem. C* **2016**, *4* (31), 7455–7463. https://doi.org/10.1039/C6TC02301K.

(25) Bourgès, C.; Bouyrie, Y.; Supka, A. R.; Al Rahal Al Orabi, R.; Lemoine, P.; Lebedev, O. I.; Ohta, M.; Suekuni, K.; Nassif, V.; Hardy, V.; Daou, R.; Miyazaki, Y.; Fornari, M.; Guilmeau, E. High-Performance Thermoelectric Bulk Colusite by Process Controlled Structural Disordering. *J. Am. Chem. Soc.* **2018**, *140* (6), 2186–2195. https://doi.org/10.1021/jacs.7b11224.

(26) Candolfi, C.; Guélou, G.; Bourgès, C.; Supka, A. R.; Al Rahal Al Orabi, R.; Fornari, M.; Malaman, B.; Le Caër, G.; Lemoine, P.; Hardy, V.; Zanotti, J.-M.; Chetty, R.; Ohta, M.; Suekuni, K.; Guilmeau, E. Disorder-Driven Glasslike Thermal Conductivity in Colusite Cu26V2Sn6S32 Investigated by Mössbauer Spectroscopy and Inelastic Neutron Scattering.

*Phys. Rev. Mater.* **2020**, *4* (2), 25404. https://doi.org/10.1103/PhysRevMaterials.4.025404.

(27) Suekuni, K.; Shimizu, Y.; Nishibori, E.; Kasai, H.; Saito, H.; Yoshimoto, D.; Hashikuni, K.; Bouyrie, Y.; Chetty, R.; Ohta, M.; Guilmeau, E.; Takabatake, T.; Watanabe, K.; Ohtaki, M. Atomic-Scale Phonon Scatterers in Thermoelectric Colusites with a Tetrahedral Framework Structure. *J. Mater. Chem. A* **2019**, *7* (1), 228–235. https://doi.org/10.1039/C8TA08248K.

(28) Lemoine, P.; Pavan Kumar, V.; Guélou, G.; Nassif, V.; Raveau, B.; Guilmeau, E. Thermal Stability of the Crystal Structure and Electronic Properties of the High Power Factor Thermoelectric Colusite Cu26Cr2Ge6S32. *Chem. Mater.* **2019**, *32* (2), 830–840. https://doi.org/10.1021/acs.chemmater.9b04378.

(29) Pavan Kumar, V.; Supka, A. R.; Lemoine, P.; Lebedev, O. I.; Raveau, B.; Suekuni, K.; Nassif, V.; Al Rahal Al Orabi, R.; Fornari, M.; Guilmeau, E. High Power Factors of Thermoelectric Colusites Cu26T2Ge6S32 (T = Cr, Mo, W): Toward Functionalization of the Conductive "Cu–S" Network. *Adv. Energy Mater.* **2019**, *9* (6), 1803249. https://doi.org/10.1002/aenm.201803249.

(30) Pavan Kumar, V.; Guélou, G.; Lemoine, P.; Raveau, B.; Supka, A.; Al Rahal Al Orabi, R.; Fornari, M.; Suekuni, K.; Guilmeau, E. Copper-Rich Thermoelectric Sulfides: Size Mismatch Effect and Chemical Disorder in the [TS4]Cu6 Complexes of Cu26T2Ge6S32 (T = Cr, Mo, W) Colusites. *Angew. Chemie Int. Ed.* **2019**, *58* (43), 15455–15463. https://doi.org/10.1002/anie.201908579.